Three-State Thermodynamic Analysis of the Denaturation of Staphylococcal Nuclease Mutants†

John H. Carra, Elizabeth A. Anderson, and Peter L. Privalov*

Department of Biology and Biocalorimetric Center, The Johns Hopkins University, Baltimore, Maryland 21218

Received May 4, 1994; Revised Manuscript Received June 28, 1994®

ABSTRACT: Using microcalorimetry, we found an equilibrium intermediate state during the denaturation of the wild-type and five mutant staphylococcal nuclease proteins: V66L, V66W, G88V, D77A, and E75V. The presence of two distinct heat absorption peaks allowed direct measurement of the enthalpy differences between the native, intermediate, and denatured states. Conditions of low pH and high NaCl concentration facilitated observation of the intermediate, or I-state. We propose to consider the nuclease protein as composed of two subdomains, divided along the active-site cleft. The structure of the I-state apparently consists mainly of the folded β-barrel subdomain, as does that of a nuclease fragment protein [Shortle, D., & Abeygunawardana, C. (1993) *Structure 1*, 121–134]. The cooperativity of folding of the subdomains is maintained by electrostatic bonds across the active-site cleft. Removal of these bonds by the mutation D77A or E75V results in decooperation of the protein's structure and a three-state mechanism of denaturation at pH 7.0. The origins of differences in the enthalpy change of denaturation and in the *m* value of guanidinium chloride-induced denaturation with mutant nucleases are discussed in terms of this three-state mechanism.

The equilibrium folding of small globular proteins usually can be described as a single first-order phase transition between the unfolded and folded states. It is clear, however, that as a protein cannot possibly sample all of its astronomical number of potential configurations before finding the native structure (Levinthal, 1968), a pathway of folding must exist, on which lie kinetic intermediates. These intermediates may consist of folded substructures or subdomains. From the thermodynamic viewpoint, we would like to understand how stable these intermediates are, how cooperative their structure is, and how similar this structure is to that of the native state. Intermediate states of protein folding, including the molten globule, are currently a subject of intensive study (Ptitsyn, 1992; Haynie & Freire, 1993).

In this work, we use the small and well-known protein staphylococcal nuclease (149 amino acids) as a model system for the study of intermediate states. Figure 1 shows the structure of nuclease (Loll & Lattman, 1989). Previously, much other work has focused on mutations of nuclease (Shortle, 1989; Sturtevant, 1993), which are often found to result in changes in the breadth of the transition region of guanidinium chloride-induced denaturation. The width of the transition can be quantitatively expressed as an *m* value (Shortle & Meeker, 1986), where the wild-type nuclease is assigned an *m* value of 1. Mutant nuclease proteins denaturing over a broader or narrower concentration range of guanidinium chloride than the wild-type protein have, respectively, an *m* value less than 1 (m^-) or greater than 1 (m^+). Differences in *m* values have been correlated to changes in the structural content of non-native forms of nuclease existing in the presence of guanidinium chloride (Shortle & Meeker, 1989). The variation in *m* values with mutation may result from changes in the occupancy of an intermediate state populated during the process of guanidinium chloride denaturation. A decreased *m* value would then result from the increased stability of a partially structured intermediate state, and likewise an increased *m* value would result from decreased structure in that form. Guanidinium chloride-induced denaturation may therefore be a three-state process for the wild-type nuclease and some of its mutants.

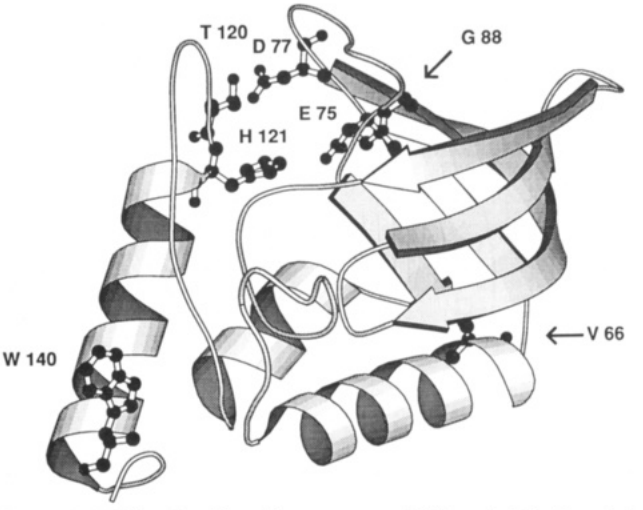

FIGURE 1: Ribbon drawing of the structure of Ca^{2+} and pdTp-liganded staphylococcal nuclease (Loll & Lattman, 1989). The figure was drawn using the program Molscript (Kraulis, 1991), with coordinates from the Brookhaven Protein Data Base (1snc.pdb). The ligands and the disordered amino acids 1–6 and 141–149 are not shown. Histidine 121, glutamate 75, tryptophan 140, threonine 120, aspartate 77, glycine 88, and valine 66 are shown in a ball-and-stick presentation.

We confirm herein the presence of an equilibrium intermediate state in the thermal denaturation of nuclease proteins. This intermediate, which we call the I-state, shares certain characteristics with a protein fragment of nuclease consisting of residues 1–136 (Flanagan et al., 1992, 1993; Gittis et al., 1993; Shortle & Meeker, 1989) and may also be similar to hypothesized intermediates in guanidinium chloride denaturation. The I-state is not the A-state of nuclease described previously (Carra et al., 1994b; Fink et al., 1993), differing from that state markedly in intrinsic fluorescence, ellipticity, temperature stability, and apparent ANS binding.

† This work was supported by NIH Grant GM 48036 and NSF Grant MCB 9118687.

* Author to whom correspondence should be addressed.

® Abstract published in *Advance ACS Abstracts,* August 15, 1994.

0006-2960/94/0433-10842$04.50/0

A structural model derived from NMR data for the 1–136 fragment of nuclease containing the mutation G88V (Shortle & Abeygunawardana, 1993) indicates that the C-terminal α-helix of this protein fragment is unfolded. The β-barrel portion of the molecule is largely intact, although possibly in a non-native conformation. The I-state appears to have roughly similar structural content, judging from CD[1] and fluorescence properties. The β-sheets are also present in an early kinetic intermediate of nuclease folding (Jacobs & Fox, 1994). This β-sheet secondary structure may therefore represent both an equilibrium and kinetic intermediate in nuclease folding.

EXPERIMENTAL PROCEDURES

Protein Preparation and Buffers. Staphylococcal nuclease A (Foggi strain) and the mutant nuclease proteins were purified, using methods previously described, from overproducing strains of *Escherichia coli* kindly provided by Drs. David Shortle and Alan Meeker (Carra et al., 1994a, Shortle & Meeker, 1989; Green & Shortle, 1993). The concentrations of protein solutions were quantified as previously described (Carra et al., 1994a,b).

The buffers used were as follows: for pH 3.0–4.1, 20 mM glycine hydrochloride; for pH 5.0–6.0, 20 mM NaOAc; for pH 7.0–8.0, 20 mM sodium phosphate. In all cases, 1 mM EDTA was included to chelate residual divalent cations.

Circular Dichroism Measurements. CD spectra were taken on a Jasco J-710 spectropolarimeter (Japan Spectroscopic Co.). A jacketed 0.05 cm circular cell was connected to a programable water bath for temperature control. Protein concentrations were kept close to 0.4 mg/mL. For melting curves, the temperature was increased at 0.5 K/min. The molar ellipticity [Θ] was calculated using an average molecular weight per amino acid residue of 112.5. Noise in the data was smoothed using the Jasco J-710 software.

Fluorescence Measurements. Fluorimetry was performed using an adapted Aminco-Bowman spectrophosphorimeter and a 1 cm rectangular cell in a water-jacketed holder (Carra et al., 1994b). The fluorescence intensity of tryptophan was measured at an emission wavelength of 340 nm with excitation at 285 nm. Protein concentrations were 0.1 mg/mL in all cases. Temperature was increased in 2 deg steps, allowing sufficient time for equilibration of the sample. The temperature of the cell holder was measured using a platinum thermistor.

Microcalorimetry. Differential scanning calorimetry was performed using a new microcalorimeter built at The Johns Hopkins University by V. Plotnikov and P. Privalov from a DASM-1M prototype (Carra et al., 1994a). The cell volume was 1.3 mL and the scanning rate was 1 K/min. Protein concentrations were between 2 and 3 mg/mL. Data were analyzed as in Privalov and Potekhin (1986), fitting the deconvoluted curves to a model of sequential transitions. Calculated heat capacities of the unfolded protein were determined as in Makhatadze and Privalov (1990). No adjustment of the enthalpy changes for ionization enthalpies was made (Carra et al., 1994a).

Partition of States. A model of two sequential transitions was applied to all of the results, where deconvolution of the excess heat capacity curves revealed two transitions. We consider the reaction:

$$N \overset{K_1}{\Leftrightarrow} I \overset{K_2}{\Leftrightarrow} D$$

where N is the native state, I is the intermediate state, D is the final denatured state achieved by heating, and K_1 and K_2 are the equilibrium constants of the first and second transitions, respectively. A partition function Z, can be written for this reaction as follows:

$$Z = 1 + K_1 + K_1K_2$$

The temperature dependence of the equilibrium constants of each transition can be calculated from the measured ΔH, T_d, and ΔC_p values (Privalov, 1979). The fractional occupancy F_i of each state can then be simply calculated as a function of temperature:

$$F_N = 1/Z \qquad F_I = K_1/Z \qquad F_D = K_1K_2/Z$$

RESULTS

Previous calorimetric investigations of staphylococcal nuclease from this laboratory and others (Carra et al., 1994a; Griko et al., 1988; Tanaka et al., 1993) have considered its thermal denaturation only as a two-state phenomenon. We have now found that this denaturation can sometimes be a three-state process, especially for mutant nucleases. Figure 2A shows calorimetric melting profiles of the mutant nuclease V66L, where the buried valine at position 66 (Figure 1) has been substituted for leucine (Shortle & Meeker, 1986). The stability of the protein has been changed by varying pH in the presence of 100 mM NaCl, 20 mM buffer (see Experimental Procedures), and 1 mM EDTA. As the pH is reduced from 7.0 to 3.8, an extended shoulder in the latter part of the curve becomes prominent. This shoulder represents a second endothermic transition. The melting of the V66L mutant protein therefore clearly is not a two-state phenomenon, at least not at pH values below 7.0. V66L has an m value for guanidinium chloride denaturation of 0.82 and is classified as an m^- mutant (Shortle & Meeker, 1986).

In Figure 2B, the pH of the experiments has been kept constant at 3.8, while the added NaCl concentration has been varied from 0 to 100 to 500 mM. The peak of heat absorption is largest and sharpest at 0 mM NaCl. At 500 mM NaCl, the single sharp peak has divided into two well-separated peaks, indicating the existence of two transitions. The increasing salt concentration has caused the first peak to shrink backward in size and temperature of denaturation and the second peak to shift to higher temperatures (Table 1). Both endothermic transitions are mostly reversible, allowing the application of equilibrium thermodynamics. The absolute values of the native state heat capacities in Figure 2A,B show some scatter along the ordinate axis; they have an error in measurement of approximately ± 3 kJ K^{-1} mol^{-1}.

Values for the enthalpies, entropies, and denaturation temperatures of the transitions are given in Table 1. These were obtained by the subtraction of linearly extrapolated heat capacities of the native and denatured states from the heat capacity data, followed by deconvolution of the resulting excess heat capacity ($\langle C_p \rangle$) curves (Biltonen & Freire, 1978; Privalov & Potekhin, 1986). This deconvolution decomposes the excess heat capacity curves into the minimum number of transitions necessary to describe the heat absorption observed. In the case of the V66L mutant, the deconvolution yielded two transitions in the pH range 3.8–7.0, but only a single transition at pH 8.0. A decrease in pH causes the denaturation process of V66L to shift from two-state to three-state character.

[1] Abbreviations: C_p, heat capacity; $\langle C_p \rangle$, excess heat capacity; T_d, denaturation temperature; CD, circular dichroism; ANS, 8-anilino-1-naphthalenesulfonic acid; pdTp, deoxythymidine 3′,5′-bisphosphate.

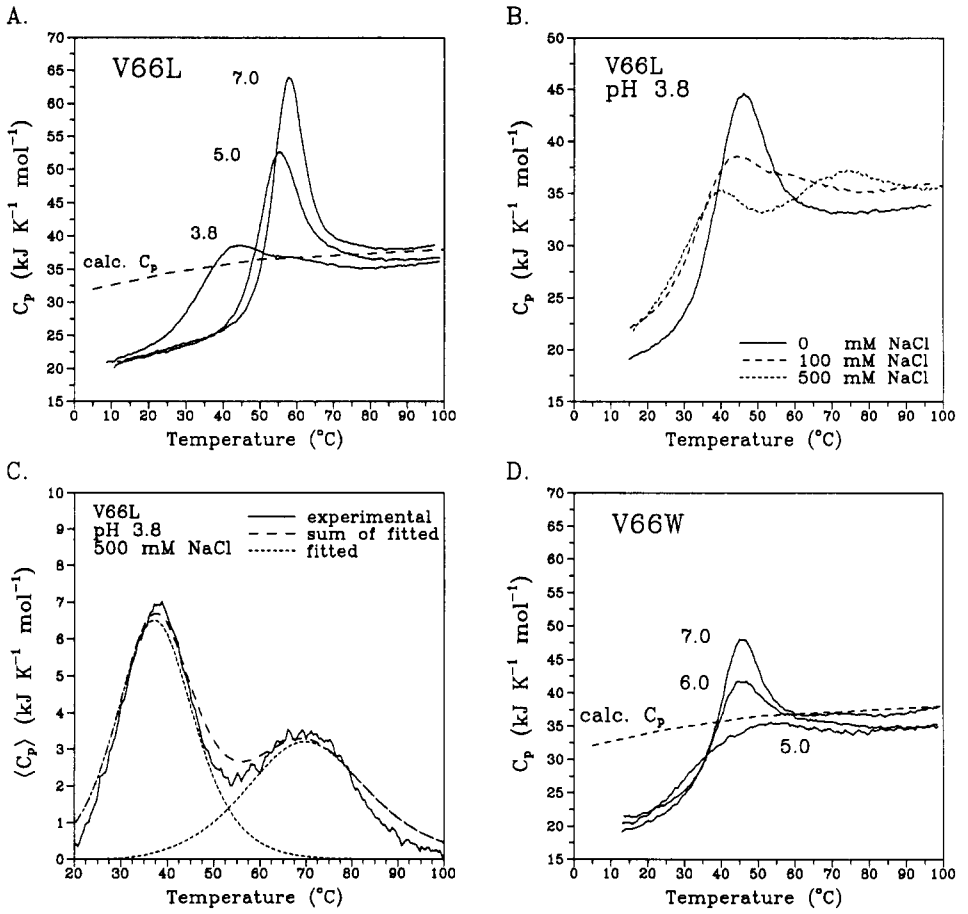

FIGURE 2: Differential scanning microcalorimetry. (A) V66L nuclease at pH 7.0, 5.0, and 3.8, as indicated on the figure. NaCl was added at 100 mM in all cases. The dashed line is the calculated heat capacity of a hypothetical fully unfolded nuclease determined according to Makhatadze and Privalov (1990). (B) V66L nuclease at pH 3.8 with varying NaCl concentrations, as indicated on the figure. (C) The excess heat capacity function of V66L nuclease at pH 3.8 and 500 mM added NaCl. The experimental results are shown along with two fitted transitions and their sum, as indicated on the figure. (D) V66W nuclease at pH 7.0, 6.0, and 5.0, with 100 mM added NaCl. The dashed line is the calculated heat capacity of a hypothetical fully unfolded V66W nuclease.

Another m^- mutant, G88V ($m = 0.78$; Green & Shortle, 1993), gives calorimetric results very similar to those for the V66L protein (Table 1).

Figure 2C shows the results of deconvolution and fitting for the V66L protein at pH 3.8 and 500 mM NaCl. In the absence of added NaCl, the two transitions are tightly linked and overlap extensively. At 500 mM NaCl, the two transitions are fairly well-separated and essentially independent. At higher pH values the effect of salt decreases, until at pH 8.0 it is quite small (Table 1), and no second peak can be found.

The deconvoluted excess heat capacity curves were fit to a model of two sequential first-order transitions, describing a three-state process of denaturation through an intermediate. A model of two independent transitions, as might be applied to a protein of two noninteracting domains, did not fit the data well for V66L at pH 3.8 and salt concentrations less than 100 mM NaCl. At higher salt concentrations, there was no difference between the results of fitting to sequential (dependent) or nonsequential (independent) models. This is as would be expected when two transitions are well-separated in temperature. The fact that a latent heat of melting of the intermediate is observed means that its transition to the denatured state is a first-order and not a second-order process. Second-order phase transitions have been proposed from theory for molten globule intermediates (Shakhnovitch & Finkelstein, 1989).

In Figure 2D are plotted the results of scanning calorimetry on another mutant protein, V66W. Deconvolution of its excess heat capacity functions reveals that it also denatures through an intermediate (Table 1). As with the V66L mutant, the effects of pH are different on the two transitions. The first transition from the native state to the intermediate is sensitive to pH in the range from 7.0 to 5.0, while the second transition from the intermediate to the final denatured state appears not to be sensitive to pH. As a result, the first transition of the curves of Figure 2D shrinks with decreasing pH, while the latter transition becomes unmasked. As pH is decreased below 3.0, the protein goes entirely to the denatured state and no melting peaks are observed (data not shown). The effects of salt on the V66W protein at pH 6.0 are similar to those for the V66L protein, with the T_d of the second transition increasing with the NaCl concentration (Table 1). Guanidinium chloride-induced denaturation of the V66W protein measured by circular dichroism or tryptophan fluorescence is biphasic (Gittis et al., 1993), pointing to the presence of an intermediate state in that process.

The fractional occupancy of the native, intermediate, and denatured states as a function of temperature can be calculated using a simple partition function (see Experimental Procedures) once the ΔH, T_d, and ΔC_p values of both transitions are known. This has been done in Figure 3A for V66L nuclease at pH 3.8 and 500 mM NaCl, where the intermediate is relatively stable. ΔC_p values of 4 ± 1 kJ K^{-1} mol^{-1} for the first transition and 1 ± 1 kJ K^{-1} mol^{-1} for the second transition were estimated directly from the heat capacity curve obtained under these conditions. Errors in the ΔH values (estimated

Table 1: Calorimetric Results of Nuclease Denaturation

pH	[NaCl] (mM)	T_d[a] (peak 1)	T_d[a] (peak 2)	ΔH_{cal}[b] (total)	ΔH_{fit}[b] (peak 1)	ΔH_{fit}[b] (peak 2)	ΔS[c] (peak 1)	ΔS[c] (peak 2)	fit[d] (error)
					Mutant V66L				
3.8	0	45.1	45.7	286	157	133	0.49	0.42	0.06
3.8	20	41.3	45.6	239	140	108	0.44	0.34	0.010
3.8	50	38.1	49.1	239	141	102	0.45	0.32	0.008
3.8	100	40.7	53.2	226	141	96	0.45	0.30	0.013
3.8	150	37.9	58.7	231	145	102	0.47	0.31	0.017
3.8	200	37.9	62.5	240	145	108	0.47	0.32	0.014
3.8	300	37.8	65.6	248	148	117	0.48	0.34	0.011
3.8	400	38.9	70.9	233	145	116	0.46	0.34	0.025
3.8	500	37.6	70.8	226	143	112	0.46	0.32	0.024
4.1	100	44.5	56.7	302	174	130	0.55	0.39	0.010
5.0	100	55.8	60.3	320	232	99	0.71	0.30	0.009
6.0	100	59.5	59.4	387	265	120	0.80	0.36	0.009
7.0	100	59.8	54.7	345	300	52	0.90	0.16	0.009
8.0	100	57.1		339	342		1.04		0.018
8.0	500	57.7		305	315		0.95		0.026
					Mutant G88V				
4.1	100	45.2	58.6	239	153	95	0.48	0.29	0.010
5.0	100	55.0	62.7	302	222	89	0.68	0.26	0.013
6.0	100	57.5	65.7	360	276	91	0.83	0.27	0.013
7.0	100	58.4	64.8	339	291	58	0.88	0.17	0.027
					Wild-Type				
4.1	0	47.1	54.0	277	252	33	0.79	0.10	0.021
4.1	100	42.0	48.3	253	181	78	0.57	0.24	0.010
4.1	500	41.0	69.7	278	202	92	0.64	0.27	0.018
7.0	100	54.1		324			0.99		0.044
					Mutant V66W				
6.0	0	47.8	43.0	250	170	82	0.53	0.26	0.009
6.0	100	45.3	60.0	213	176	51	0.55	0.15	0.012
6.0	200	43.7	71.6	210	174	54	0.55	0.16	0.018
6.0	300	43.4	77.9	195	164	56	0.52	0.16	0.021
6.0	400	43.5	66.3	219	158	74	0.50	0.22	0.016
6.0	500	42.8	67.5	217	150	79	0.48	0.23	0.011
7.0	100	46.3	50.8	280	208	74	0.65	0.23	0.012
					Mutant D77A				
5.0	100	40.7	60.3	198	151	68	0.48	0.21	0.028
7.0	0	44.1	71.4	256	206	83	0.65	0.24	0.037
7.0	100	43.4	72.6	274	210	88	0.66	0.25	0.024
7.0	500	45.3	69.7	286	217	88	0.68	0.26	0.016
					Mutant E75V				
5.0	100	40.1	65.49	198	152	68	0.48	0.20	0.029
6.0	100	45.1	75.2	257	218	62	0.69	0.18	0.022
7.0	100	47.5	60.8	292	238	66	0.74	0.20	0.022

[a] Denaturation temperature in °C. Errors are ±0.5 K. [b] In kJ mol^{-1}. Errors in enthalpies are approximately ±10%. [c] In kJ K^{-1} mol^{-1}. Errors are approximately ±10%. [d] Mean square deviation of the fitted curves.

at ±10%) and in the heat capacity increment values are significant and will cause increasing error in the fractional population of states as one moves farther from the denaturational temperatures. From Figure 3A, we can see that the predicted fraction of the protein population in the I-state reaches a maximum of approximately 85% at 53 °C.

The intermediate has a far-UV CD spectrum indistinguishable from that of the heat-denatured protein at 95 °C (Figure 3B), indicating that the I-state has lost most or all of the native state's α-helix content. The high temperatures and salt concentrations used produce a large amount of noise at shorter wavelengths, preventing data analysis below 206 nm. Similar spectra have been observed for acid-denatured nuclease at pH 2.8 and 25 °C (Chen et al., 1991), where deconvolution yielded a result of 52% β-sheet, 4% turn, 44% random coil, and negligible α-helix. The nature of the structures that gives rise to this ellipticity is quite unclear, however, as no melting endotherm is observable under these conditions. Circular dichroism does not appear to be able to distinguish the presence of β-sheets from more disordered heat-denatured conformations. Therefore, the β-sheet content of the intermediate cannot be ascertained by this method.

Figure 4A follows the changes in Θ_{222} and in fluorescence from Trp_{140} for the V66L protein under the same conditions as used in Figure 3B. The sum of the fractions of the intermediate and denatured states, calculated from calorimetric data as in Figure 3A, is also graphed. While there is some separation along the temperature axis between the transitions observed by these three techniques, this is within experimental error. The three parameters essentially change in parallel, which means that both the changes in Θ_{222} and in Trp_{140} fluorescence monitor the first heat absorption transition, not the second transition, which occurs much later (see Figure 2B and Table 1). Tryptophan 140 lies near the end of the C-terminal α-helix (Figure 1) and is mostly buried from solvent in the native structure. Loss of its fluorescence signal during the transition to the intermediate confirms the unfolding of the C-terminal helix predicted from the CD signal.

For V66W protein at pH 6.0 and 0 mM NaCl, the ellipticity and fluorescence signals change in parallel, as in Figure 4A. Under these conditions, the two denaturational transitions overlap almost completely. Fluorescence emission from V66W protein arises from both the tryptophan at position 140 and that introduced at position 66. Both are buried in the native

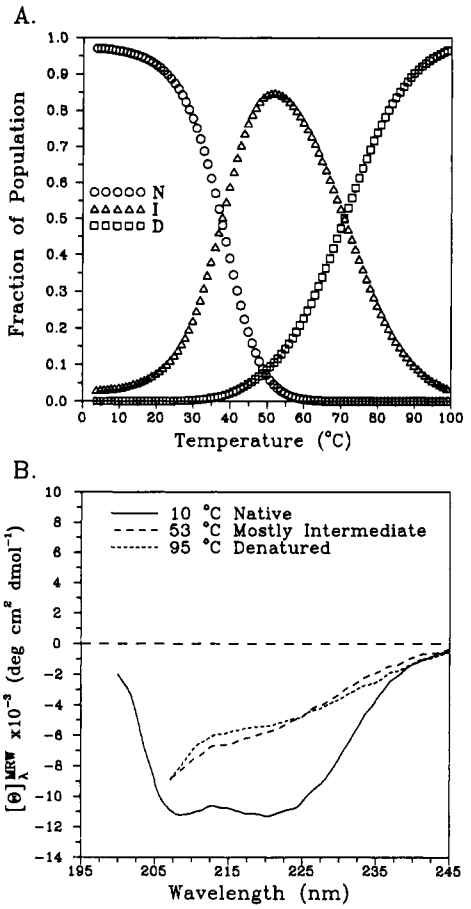

FIGURE 3: (A) Native, intermediate, and denatured states as fractions of the protein population during the melting of V66L nuclease at pH 3.8 and 500 mM NaCl. The partition of states was calculated as described in the Experimental Procedures, using data from Table 1 and ΔC_p values of 4 ± 1 and 1 ± 1 kJ K^{-1} mol^{-1} for the first and second transitions, respectively. (B) Far-UV circular dichroism wavelength scan of V66L nuclease at pH 3.8 and 500 mM NaCl, at temperatures of 10 °C, where the protein is in the native state, 53 °C, where it is calculated to be 85% I-state, and 95 °C, where it is in the denatured state.

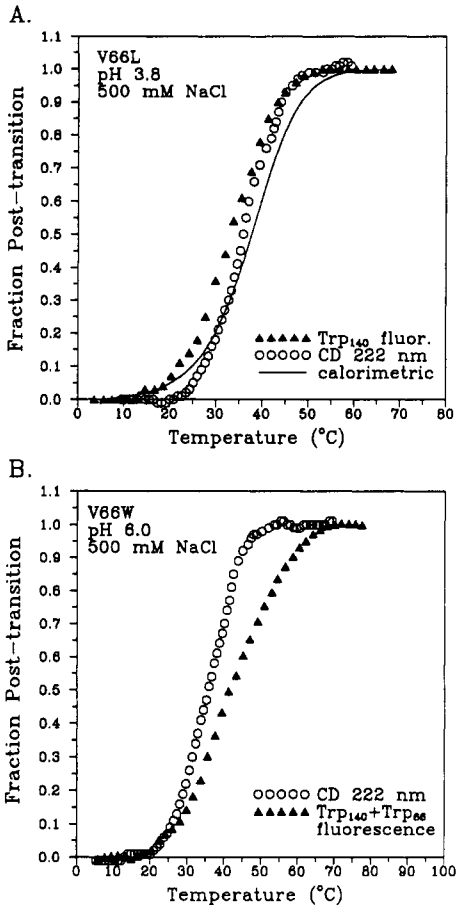

FIGURE 4: (A) Posttransitional fraction of the V66L nuclease population at pH 3.8 and 500 mM NaCl, calculated from tryptophan fluorescence emission at 340 nm (▲), CD at 222 nm (O), or from calorimetric data as in Figure 3A. The sum of the intermediate and denatured states calculated from calorimetric data is graphed as a solid line. The posttransitional fraction of the population was calculated from CD and fluorescence measurements after the subtraction of linearly fitted and extrapolated pre- and posttransitional baselines from the raw data. (B) Posttransitional fraction for the V66W protein at pH 6.0 and 500 mM NaCl, graphed as in part A.

state (Gittis et al., 1993). If we perform the same experiment on the V66W protein at pH 6.0 and 500 mM NaCl, however, the CD and fluorescence signals diverge markedly in the latter half of the curves (Figure 4B). This divergence must result from a change in fluorescence associated with the second heat absorption peak, which at this higher salt concentration is well-separated from the first transition (Table 1). By comparison to the result obtained with V66L, which has Trp_{140} but lacks a tryptophan at position 66 and does not show the divergence of CD and fluorescence signals, the latter half of the fluorescence signal change of Figure 4B must be assigned to Trp_{66}. It has previously been found by Gittis et al. (1993) that the nuclease fragment V66W 1–136 shows a sigmoidal decrease in fluorescence from Trp_{66} with increasing temperature. This transition was proposed to be approximately first-order in nature, which agrees with our calorimetric result on the full-length V66W protein.

Unlike some other non-native protein forms (Semisotnov, 1991), including the A-state of staphylococcal nuclease (Carra et al., 1994b; Fink et al., 1993), the I-state apparently does not bind the hydrophobic fluorescent dyes ANS or Nile Red, as no significant increase in fluorescence from these compounds was found during the denaturation of the V66L protein at pH 3.8 and 500 mM NaCl (data not shown).

Previously, we observed that the wild-type nuclease showed an anomalously low ΔH of denaturation at pH 4.1 (Carra et al., 1994a). We attributed this enthalpy deficit to the occurrence of incomplete thermal unfolding at low pH. In those experiments, we did not consider it necessary to include EDTA in the buffer at pH 4.1, as it had been found previously that Ca^{2+}, which specifically binds to and stabilizes nuclease at neutral pH, had no effect at pH 4.0 (Calderon et al., 1985). We observed only one peak in the heat capacity function. We now have found that when 1 mM EDTA is included to chelate trace quantities of divalent cations, two endothermic transitions are present for the wild-type nuclease at pH 4.1 and 500 mM NaCl (Table 1). Trace quantities of divalent cations apparently stabilize the intermediate state, yielding an initial transition to the intermediate and not the denatured state. The presence of either NaCl above 100 mM, or low concentrations of calcium, will give the intermediate (data not shown). In the absence of both divalent metals and NaCl, the intermediate is unstable, and the melting of nuclease at pH 4.1 is almost a two-state process, going directly from the native state to the denatured state. EDTA at 0.1 mM is sufficient to remove these residual divalent cations, and higher concentrations of EDTA (to 5 mM) do not further stabilize the native state (data not shown), indicating that EDTA binding to the protein is not the origin of its influence. The

effects of metal salts on the intermediate state will be explored in more depth in a future publication.

It is now clear that the anomalously low ΔH values at pH 4.1 that we measured previously were indeed due to incomplete unfolding. This incompletely unfolded form can now be identified as a discrete intermediate state because an endothermic transition has been found to separate it from the denatured state. The enthalpy of melting of the wild-type nuclease I-state (Table 1) is found to be 78 kJ mol^{-1} (±10%) at a T_d of 48.3 °C. This number is very close to the estimate of Carra et al. (1994a) obtained indirectly for the enthalpy of residual structure remaining after the major endothermic peak. That value was 70 kJ mol^{-1} at 42 °C. A correction of 1 ± 1 kJ K^{-1} mol^{-1} (an estimate of the ΔC_p of the second transition) should be applied for the difference in denaturation temperatures.

In the structural model of the nuclease fragment G88V 1–136 presented by Shortle and Abeygunawardana (1993), the β-barrel portion of the protein is folded, while the long C-terminal α-helix is disordered. The states of the other two α-helices are unclear. This result suggested to us that the nuclease protein can usefully be considered as two interacting subdomains: one mainly a β-barrel and the other mainly α-helical. The denaturation of individual subdomains could produce the two endothermic transitions observed. The protein's active-site cleft is an obvious structural divider (Figure 1). A network of hydrogen bonds stretches across this cleft, some of which involve charged side chains (Hynes & Fox, 1991; Loll & Lattman, 1989). It may be reasonable to predict that removal of these bonds by mutation of the residues involved would result in decooperation of the subdomains and a three-state denaturation mechanism.

To test the above hypothesis, we have studied two nuclease proteins mutated in residues forming bonds across the active-site cleft: D77A and E75V (Figure 1). The side chain of aspartate 77 makes two hydrogen bonds across this cleft to threonine 120: one to the side-chain hydroxyl group, and one to the peptide nitrogen. The bond to the peptide nitrogen has been found to be particularly strong (Loh & Markley, 1994). Figure 5A shows the result of scanning calorimetry on the D77A protein at pH 7.0 and 100 mM NaCl. Two peaks are present, the first of which has over twice the enthalpy of the second (Table 1). The mutation of aspartate 77 to alanine has indeed resulted in a three-state denaturation. The two peaks are well-separated, suggesting that they are essentially independent. These two transitions at pH 7.0 show little or no dependence on NaCl (Table 1). The inset of Figure 5A shows repeated scans of the D77A protein to 80 °C, also at pH 7.0. Both transitions are still present even after seven cycles, indicating that they are effectively reversible.

In Figure 5B are plotted the results for the E75V protein at various pH values and 100 mM NaCl. Glutamate 75 is involved in a salt bridge bond to histidine 121 across the active-site cleft (Loll & Lattman, 1989). At pH 4.1, the heat capacity function of the E75V protein increases in two well-pronounced steps, clearly revealing the presence of an intermediate. A weak second transition is observable at pH 7.0 and 5.0 as well. The mutation of glutamate 75 to valine has also resulted in a three-state mechanism of denaturation.

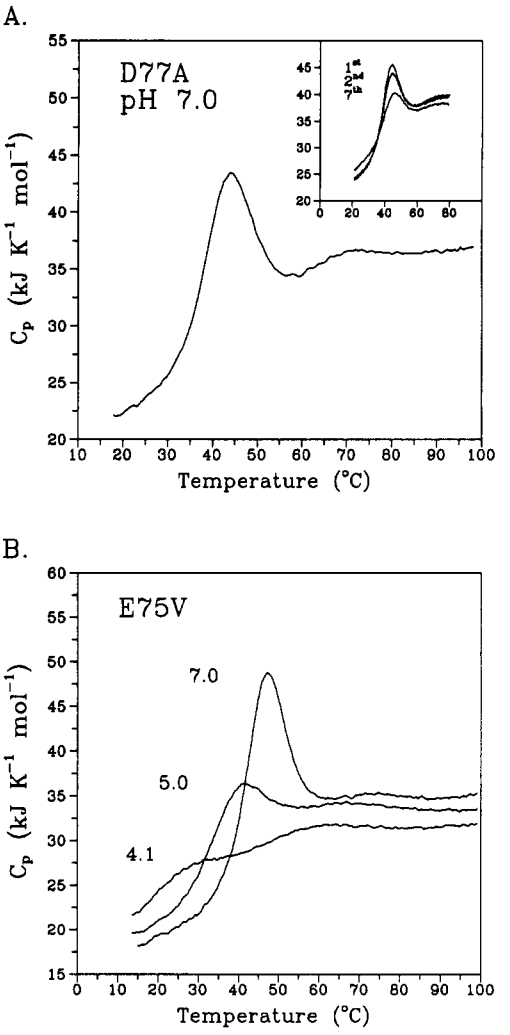

FIGURE 5: (A) Scanning calorimetry on D77A nuclease at pH 7.0 and 100 mM NaCl. The inset shows repeated scans of D77A nuclease at pH 7.0 and 100 mM NaCl. The protein was heated to 80 °C and then cooled and rescanned repeatedly. (B) Scanning calorimetry on E75V nuclease at pH 7.0, 5.0, and 4.1, with 100 mM NaCl.

DISCUSSION

The existence of two subdomains in staphylococcal nuclease is not a new idea, having first been suggested in the early work of Anfinsen (1972). The assignment of the I-state to the β-barrel subdomain is supported by the loss of α-helical content determined from CD and Trp_{140} fluorescence, as well as its fluorescence properties, which are similar to those of the nuclease fragment V66W 1–136 (Gittis et al., 1993). The structure of the fragment G88V 1–136 is known to consist mainly of the β-barrel (Shortle & Abeygunawardana, 1993). The transitions from the native state to the intermediate and from the intermediate to the denatured state are largely reversible (Figure 5A, inset), and good fits are obtained to a model of sequential transitions of a monomer (Figure 2C). This indicates that the intermediate observed is not an indiscriminately aggregated form or a dimeric form, in contrast to the intermediate state of the CheY protein (Filimonov et al., 1993). The absence of a concentration dependence of the first transition observed by fluorescence at 0.1 mg/mL protein, by circular dichroism at 0.4 mg/mL, or by calorimetry at ~2.5 mg/mL also supports the conclusion that the protein has not significantly oligomerized in going to the intermediate.

A model of staphylococcal nuclease composed of two subdomains is diagramed simplistically in Figure 6. The subdomain containing the long C-terminal α-helix is labeled A and the β-barrel subdomain is labeled B. A and B are linked covalently by the polypeptide chain and interact in the native state through bonds shown as dashed lines. The elimination of these interactions by mutations such as D77A or E75V results in decooperation of the global structure and

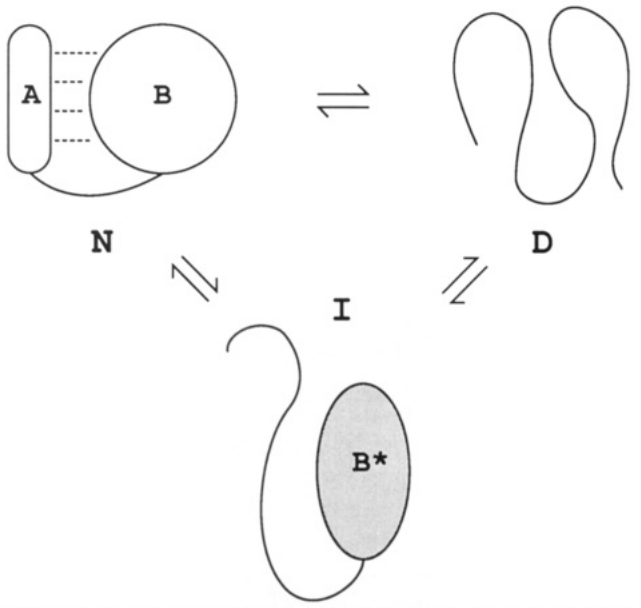

FIGURE 6: Cartoon depicting the native, intermediate, and denatured states. The protein is shown divided into two subdomains A and B.

denaturation through intermediate states. In the intermediate state, the A subdomain has unfolded, along with most or all of the protein's α-helix content. The conformation of the B subdomain after the A subdomain has melted may be significantly altered; therefore, this part of the protein has been labeled B* in the intermediate. After the second transition, leading to the D state, the whole protein has become denatured, although even now it may not exist as a true random coil (Carra et al., 1994a; Wu et al., 1994).

The enthalpy and free energy changes of unfolding the I-state are perhaps best estimated by the results for the D77A protein, because in this case two well-separated peaks are obtained at pH 7.0, without the complicating factors of low pH and salt dependency. The substitution of alanine for aspartate is relatively conservative, as it only removes a carboxyl group. While the ΔH of the second transition of the D77A protein at pH 7.0 and 100 mM NaCl is 2.4 times smaller than that of the first transition (Table 1), its ΔG at 20 °C can be calculated as 9.2 ± 2 kJ mol^{-1}, compared to 10 ± 2 kJ mol^{-1} for the first transition. ΔC_p values at pH 7.0 of 6 ± 1 and 1 ± 1 kJ K^{-1} mol^{-1} for the first and second transitions, respectively, were estimated from the calorimetric curve and applied to the data of Table 1 for this calculation. The energetic contribution of the B subdomain to folding at 20 °C is comparable to that of the rest of the protein.

Lowering of the pH from 7.0 to 3.8 strongly affects the first transition of the nuclease proteins (Table 1, Figure 2D), but not the second transition. The three-state character of denaturation is more prominent at low pH because of the selective destabilization of part of the native state's structure by acidic pH.

Increasing the NaCl concentration actually has two distinct effects on the denaturation of nuclease at low pH. The first effect is to reduce the T_d of the first transition and, as a result, the total enthalpy change of denaturation, ΔH_{cal} (Table 1). This effect occurs mainly between 0 and 200 mM NaCl. The second effect of salt is to increase the T_d of the second transition, which occurs throughout the range of 0–500 mM NaCl and is mainly entropic in nature (Table 1). Similar effects of salt have been observed before for intermediate forms of other proteins at low pH (Goto et al., 1990; Goto & Nishikiori, 1991; Kuroda et al., 1992) and have been attributed to binding of the anion species. In this case, however, it is not yet clear whether the effects of NaCl are due to the binding of cation or anion. They may also be due to the electrostatic screening of repelling charges on the intermediate state.

Mutations have a large effect on the occupancy of the I-state. The mutations V66L and G88V stabilize both the I-state and the native state relative to the denatured state. These mutations have also been observed to increase structure in the 1–136 fragment of nuclease (Flanagan et al., 1993; Shortle & Abeygunawardana, 1993; Shortle & Meeker, 1989). Considering that the location of position 66 is far from the interface between subdomains (Figure 1), it is difficult to see how mutations at that site may affect the interaction between subdomains, although formally this cannot be ruled out. It is more likely that the V66L and G88V proteins show three-state denaturation because the mutations stabilize the subdomain structure present in the intermediate. The mutation V66W destabilizes the native state, but appears to have less of a destabilizing effect on the intermediate, judging by the population of that state. Another substitution at position 66, V66A, has a T_d at pH 7.0 that is 11.9 K lower than that of the wild-type protein (Table 2) and shows no signs of an intermediate (Carra et al., 1994a). V66A is an m^+ mutant, with an m value of 1.10 (Shortle et al., 1990).

The occupancy of the I-state during thermal denaturation seems to correlate with the m^- phenotype of guanidine denaturation. All of the m^- mutants studied (V66L, V66W, G88V, E75V, and D77A) exhibit the intermediate at pH 7.0 and 100 mM NaCl, while the wild-type protein requires a lower pH of 4.1 and higher salt concentrations to show an intermediate. It remains to be seen if this m value correlation to the thermal denaturation intermediate will hold for a larger collection of mutants. Nevertheless, the data so far strongly suggest that the origin of the m^- characteristic lies in a three-state mechanism of denaturation by guanidinium chloride. It is possible that the wild-type nuclease also unfolds through an intermediate with the addition of denaturant. Thus, the m^+ behavior may be ascribed to reduced stability of the guanidinium chloride-induced intermediate relative to the case of wild-type protein.

It should be noted that while m^- mutations can stabilize or destabilize the native state of nuclease, m^+ mutations invariably destabilize it (Shortle & Meeker, 1986; Shortle et al., 1990; Green et al., 1992; Sondek & Shortle, 1992; Green & Shortle, 1993). It could be proposed that m^+ behavior arises from destabilization of the B subdomain, which will weaken both the native and intermediate states relative to the reference denatured state (e.g., V66A protein). m^- behavior may arise by decooperation of the subdomains by mutations such as D77A and E75V, by reduction of the intrinsic stability of the A subdomain, or by stabilization of the B subdomain specifically by mutations such as V66L and G88V. The first and second classes of mutations will result in a less stable native state, while the third will yield a more stable native state. The V66W protein appears to occupy the intermediate state because the N-state has a more stringent objection to this substitution than the I-state.

The effects of mutations on the energetics of protein folding have, for many years, presented perplexing difficulties. As has been pointed out by Sturtevant (Tanaka et al., 1993; Sturtevant, 1993, 1994), mutations often are found to have large effects on the ΔH of a protein's denaturation. The structural perturbations induced in the native state by substitution mutations are, however, believed to be usually small [see Lattman and Rose (1993)]. The enthalpy and

Table 2: Comparison of Mutant Enthalpies and Free Energies

protein	m^a	$\Delta T_d{}^b$	$\Delta\Delta G$ (GuHCl)^c	$\Delta\Delta G_{tot}$ (calor)^d	$\Delta\Delta G_1{}^e$	$\Delta H_{tot}{}^f$	$\Delta H_1{}^g$	$\Delta\Delta H_{tot}{}^h$
wild-type	1.0	0	0	0	0	295	295	0
V66L	0.82[i]	5.7	−0.8[i]	3.7	0.1	289	241	−6
V66W	(0.98, 0.36)[j]	−7.8	(−13, −15)[j]	−4.9	−10	303	230	8
V66A	1.10[k]	−11.9	−9.2[k]	−9.0	−9.0	303	303	8
G88V	0.78[l]	4.3	−3.8[l]	3.6	−1.0	284	241	−11
E75V	0.79[l]	−6.6	−9.7[l]	−2.3	−7.7	309	253	14
D77A	(m^-)[m]	−10.7	−13[n]	−1.5	−11	315	250	20

[a] The m value for denaturation by guanidinium chloride. Data were from the literature as cited. [b] The calorimetrically determined difference in denaturation temperature between a mutant and wild-type protein at pH 7.0. Data is for peak 1 from Table 1. Errors are ±0.5 K. [c] Data were from the literature for the difference in free energy of unfolding between a mutant and wild-type protein at 20 °C in kJ mol^{-1}, as determined by guanidinium chloride denaturation, assuming a two-state transition. [d] The difference in total free energy of unfolding of a mutant protein versus wild-type, in kJ mol^{-1}, measured calorimetrically at pH 7.0. Results were extrapolated to 20 °C from data in Table 1 using ΔC_p values of 6 ± 1 and 1 ± 1 kJ K^{-1} mol^{-1} for the first and second transitions, respectively. For wild-type and V66A proteins, where only one transition was observed at pH 7.0, ΔC_p was taken as 7 kJ K^{-1} mol^{-1}. Errors on free energies are estimated at ±2 kJ mol^{-1}. [e] The free energy difference at 20 °C between the first endothermic transition of a mutant protein and the total free energy of unfolding of the wild-type protein, in kJ mol^{-1}. [f] The extrapolated total enthalpy of unfolding at 50 °C, in kJ mol^{-1}. [g] The extrapolated enthalpy at 50 °C of the first endothermic transition, in kJ mol^{-1}. [h] The difference in total enthalpy of unfolding between a mutant and wild-type protein at 50 °C, in kJ mol^{-1}. [i] Shortle & Meeker, 1986. [j] Gittis et al., 1993. The two values were derived from different halves of a biphasic denaturation curve. [k] Shortle et al., 1990. [l] Green & Shortle, 1993. [m] Personal communication from Dr. David Shortle. [n] Loh & Markley, 1994.

heat capacity changes of unfolding have been found to be proportional to the surface areas buried from water in the native state (Makhatadze & Privalov, 1993; Privalov & Makhatadze, 1993). If these two points are accepted, small changes in the native state cannot be responsible for the large enthalpy differences found with mutations. These energetic differences must arise from major changes in a non-native form of the protein, as has been proposed before (Dill & Shortle, 1991; Shortle & Meeker, 1986).

A crucial difference between this study and much previous work done on nuclease is that we define the intermediate state separately from the denatured state. Historically, the denatured state has been defined as the form adopted by a protein after loss of its activity due to the variation of some environmental condition (Tanford, 1968). For the purposes of thermodynamic investigation, it is preferable to specify the denatured state as a form that has lost all significant elements of native structure. Therefore, we exclude the I-state from the denatured state. This choice of definitions is critical to the thermodynamic parameters measured. For any mutant nuclease protein that undergoes a three-state denaturation through the intermediate described here, enthalpy or free energy changes obtained from Trp_{140} fluorescence or far-UV circular dichroism data will omit the contribution of the second endothermic transition. The resulting values may be expected to represent only the transition from the native to the intermediate state, i.e., the melting of only one of the two subdomains, and not the total enthalpy or free energy change of unfolding.

In the paper of Shortle et al. (1988), it was reported that the apparent enthalpy change of denaturation, measured using fluorescence from Trp_{140}, was significantly less for V66L and three other m^- mutant proteins compared to the wild type at an equivalent T_d. The lower apparent enthalpy changes were considered to result either from changes in the structure of the heat-denatured state or from the presence of an intermediate state. From the results presented here, it now seems that the apparent enthalpy changes of V66L were found to be low because this denaturation is a three-state process, in which fluorescence changes monitor only the first transition.

Table 2 lists the $\Delta\Delta H$ values for each mutant studied here versus the wild-type protein at pH 7.0 and 50 °C. We do not find very large differences in the enthalpy of denaturation between the mutants and the wild-type protein, as long as the enthalpy of the second endothermic transition is included ($\Delta\Delta H_{tot}$). If the enthalpy of the second transition is not taken into account (ΔH_1), significant differences are present. We have chosen to present ΔH values calculated at 50 °C in order to minimize errors of extrapolation (Table 2).

A three-state denaturation mechanism provides an explanation for the paradoxical finding that some m^- mutants, such as V66L and G88V, have higher T_d values than the wild-type protein under the same conditions (Shortle et al., 1988; Tanaka et al., 1993), but are calculated to be less stable than wild type at 20 °C using guanidinium chloride denaturation data from fluorescence measurements, assuming a two-state transition (Shortle & Meeker, 1986). The difference in free energy of unfolding for V66L nuclease compared to wild-type nuclease at 20 °C given by Shortle and Meeker (1986) is −0.8 kJ mol^{-1} (less stable than wild type; Table 2). If we calculate the $\Delta\Delta G$ at 20 °C of V66L from the data in Table 1 at pH 7.0, we find values of 0.1 kJ mol^{-1} for the first transition by itself ($\Delta\Delta G_1$, Table 2) and 3.7 kJ mol^{-1} for both transitions together ($\Delta\Delta G_{tot}$). The value obtained for the first transition alone is within an error of ±2 kJ mol^{-1} of that obtained by fluorescence measurements. The significantly higher value of $\Delta\Delta G_{tot}$ is in accord with the V66L mutant protein's 5.7 K higher T_d value at pH 7.0 (T_d of first transition; Table 2).

Conclusions about the energetics of the G88V protein can be made similar to those for the V66L protein (Table 2). The differing conclusions from calorimetric and fluorescence studies about the energetics of V66L and G88V arise from the different definition of the "denatured state" used in this study versus those of Shortle and Meeker (1986) and Green and Shortle (1993). There is no essential disagreement when the appropriate reference states are considered.

An alternative explanation for these differing $\Delta\Delta G$ values is that the V66L and G88V proteins have lesser ΔC_p values (Shortle et al., 1988). Our calorimetric scans, however, reveal no significant difference in the total ΔC_p between V66L or G88V and wild-type protein. A previous calorimetric study (Tanaka et al., 1993) also included the mutants V66L and G88V, but in that work no deconvolution was performed, and the data at all pH values were fit to only a two-state model. The calorimetric ΔH values obtained were less than those of the wild-type protein at an equivalent T_d. The T_d values for both V66L and G88V were also found to be higher than that of the wild-type protein at pH 7.0.

The mutants E75V and D77A present particularly interesting examples of the energetic effects of mutations. While

these mutants yield relatively small reductions in the $\Delta\Delta G_{tot}$ of unfolding (–2.3 and –1.5 kJ mol^{-1}, respectively), they produce much larger effects on $\Delta\Delta G_I$ (–7.7 and –11 kJ mol^{-1}). The large negative values of $\Delta\Delta G_I$ indicate that these two mutants will occupy the intermediate state much more readily than the wild-type protein. This, we believe, is a result of the decooperation of subdomains by the removal of crucial linking bonds.

Occupancy of a partly folded state may commonly be the case, under physiological conditions, for a protein that has suffered a severely destabilizing mutation. Inactivation of a protein by a substitution mutation affecting structure is unlikely to result in a significant population of fully unfolded protein under conditions that normally support native states. The equilibrium between the native state and the conformation nearest to it in free energy, yet inactive, is the physiologically relevant balance in this case. The energy difference between native and intermediate states is a crucial factor in the maintenance of the fully folded form and is essential to the specification of a native protein structure by design or evolution.

ACKNOWLEDGMENT

We thank Drs. David Shortle and Alan Meeker for the gift of strains of overproducing nuclease proteins and Dr. Ludwig Brand for the use of a fluorimeter.

REFERENCES

Anfinsen, C. (1972) *Biochem. J. 128*, 737–749.
Biltonen, R., & Freire, E. (1978) *Crit. Rev. Biochem. 5*, 85–124.
Calderon, R. O., Stolowich, N. J., Gerlt, J. A., & Sturtevant, J. M. (1985) *Biochemistry 24*, 6044–6049.
Carra, J., Anderson, E., & Privalov, P. (1994a) *Protein Sci. 3*, 944–951.
Carra, J., Anderson, E., & Privalov, P. (1994b) *Protein Sci. 3*, 952–959.
Chen, H., You, J., Markin, V., & Tsong, T. (1991) *J. Mol. Biol. 220*, 771–778.
Dill, K. A., & Shortle, D. (1991) *Annu. Rev. Biochem. 60*, 795–825.
Filimonov, V., Prieto, J., Martinez, J., Bruix, M., Mateo, P., & Serrano, L. (1993) *Biochemistry 32*, 12906–12921.
Fink, A., Calciano, L., Goto, Y., Nishimura, M., & Swedberg, S. (1993) *Protein Sci. 2*, 1155–1160.
Flanagan, J. M., Kataoka, M., Shortle, D., & Engelman, D. M. (1992) *Proc. Natl. Acad. Sci. U.S.A. 89*, 748–752.
Flanagan, J., Kataoka, M., Fujisawa, T., & Engelman, D. (1993) *Biochemistry 32*, 10359–10370.
Gittis, A., Stites, W., & Lattman, E. (1993) *J. Mol. Biol. 232*, 718–724.
Goto, Y., & Nishikiori, S. (1991) *J. Mol. Biol. 222*, 679–686.
Goto, Y., Calciano, L. J., & Fink, A. L. (1990) *Proc. Natl. Acad. Sci. U.S.A. 87*, 573–577.
Green, S., & Shortle, D. (1993) *Biochemistry 32*, 10131–10139.
Green, S., Meeker, A., & Shortle, D. (1992) *Biochemistry 31*, 5717–5728.
Griko, Y. V., Privalov, P. L., Sturtevant, J. M., & Venyaminov, S. Y. (1988) *Proc. Natl. Acad. Sci. U.S.A. 85*, 3343–3347.
Haynie, D., & Freire, E. (1993) *Proteins: Struct., Funct., Genet. 16*, 115–140.
Hynes, T., & Fox, R. (1991) *Proteins: Struct., Funct., Genet. 10*, 92–105.
Jacobs, M., & Fox, R. (1994) *Proc. Natl. Acad. Sci. U.S.A. 91*, 449–453.
Kraulis, P. (1991) *J. App. Crystallogr. 24*, 946–950.
Kuroda, Y., Kidokoro, S., & Wada, A. (1992) *J. Mol. Biol. 223*, 1139–1153.
Lattman, E., & Rose, G. (1993) *Proc. Natl. Acad. Sci. U.S.A. 90*, 439–441.
Levinthal, C. (1968) *Chim. Phys. 65*, 44–45.
Loh, S., & Markley, J. (1994) *Biochemistry 33*, 1029–1036.
Loll, P., & Lattman, E. (1989) *Proteins: Struct., Funct., Genet. 5*, 183–201.
Makhatadze, G. I., & Privalov, P. L. (1990) *J. Mol. Biol. 213*, 375–384.
Makhatadze, G. I., & Privalov, P. L. (1993) *J. Mol. Biol. 232*, 639–659.
Privalov, P. L. (1979) *Adv. Protein Chem. 33*, 167–241.
Privalov, P. L., & Potekhin, S. A. (1986) *Methods Enzymol. 131*, 4–51.
Privalov, P. L., & Makhatadze, G. I. (1993) *J. Mol. Biol. 232*, 660–679.
Ptitsyn, O. B. (1992) in *Protein Folding* (Creighton, T. E., Ed.) pp 243–300, W. H. Freeman and Company, New York.
Semisotnov, G., Rodionova, N., Razgulyaev, O., Uversky, V., Gripas, A., & Gilmanshin, R. (1991) *Biopolymers 31*, 119–128.
Shakhnovitch, E. I., & Finkelstein, A. V. (1989) *Biopolymers 28*, 1667–1694.
Shortle, D. (1989) *J. Biol. Chem. 264*, 5315–5318.
Shortle, D., & Meeker, A. K. (1986) *Proteins: Struct., Funct., Genet. 1*, 81–89.
Shortle, D., & Meeker, A. (1989) *Biochemistry 28*, 936–944.
Shortle, D., & Abeygunawardana, C. (1993) *Structure 1*, 121–134.
Shortle, D., Meeker, A., & Freire, E. (1988) *Biochemistry 27*, 4761–4768.
Shortle, D., Stites, W., & Meeker, A. (1990) *Biochemistry 29*, 8033–8041.
Sondek, J., & Shortle, D. (1992) *Proteins: Struct., Funct., Genet. 13*, 132–140.
Sturtevant, J. (1993) *Pure Appl. Chem. 65*, 991–998.
Sturtevant, J. (1994) *Curr. Opin. Struct. Biol. 4*, 69–78.
Tanaka, A., Flanagan, J., & Sturtevant, J. M. (1993) *Protein Sci. 2*, 567–576.
Tanford, C. (1968) *Adv. Protein Chem. 23*, 121–282.
Wu, P., James, E., & Brand, L. (1994) *Biophys. Chem. 48*, 123–133.